Neutron spectrometry—An essential tool for diagnosing implosions at the National Ignition Facility (invited)

M. Gatu Johnson, J. A. Frenje, D. T. Casey, C. K. Li, F. H. Séguin et al.

Related Articles

Validation of neutron emission profiles in MAST with a collimated neutron monitor
Rev. Sci. Instrum. 83, 10D910 (2012)

Development of the ITER magnetic diagnostic set and specification
Rev. Sci. Instrum. 83, 10D712 (2012)

Dual transmission grating based imaging radiometer for tokamak edge and divertor plasmas
Rev. Sci. Instrum. 83, 10E511 (2012)

New ion source for KSTAR neutral beam injection system
Rev. Sci. Instrum. 83, 02B112 (2012)

Operation Request Gatekeeper: A software system for remote access control of diagnostic instruments in fusion experiments
Rev. Sci. Instrum. 81, 10E124 (2010)
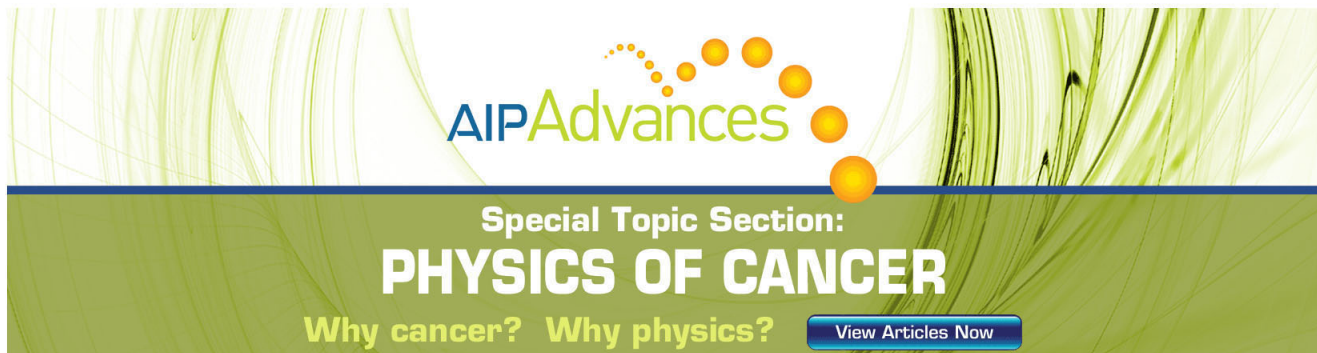
Additional information on Rev. Sci. Instrum.

Journal Homepage: http://rsi.aip.org

Journal Information: http://rsi.aip.org/about/about_the_journal

Top downloads: http://rsi.aip.org/features/most_downloaded

Information for Authors: http://rsi.aip.org/authors

Neutron spectrometry—An essential tool for diagnosing implosions at the National Ignition Facility (invited)[a]

M. Gatu Johnson,[1,b] J. A. Frenje,[1] D. T. Casey,[1] C. K. Li,[1] F. H. Séguin,[1] R. Petrasso,[1]
R. Ashabranner,[2] R. M. Bionta,[2] D. L. Bleuel,[2] E. J. Bond,[2] J. A. Caggiano,[2] A. Carpenter,[2]
C. J. Cerjan,[2] T. J. Clancy,[2] T. Doeppner,[2] M. J. Eckart,[2] M. J. Edwards,[2] S. Friedrich,[2]
S. H. Glenzer,[2] S. W. Haan,[2] E. P. Hartouni,[2] R. Hatarik,[2] S. P. Hatchett,[2] O. S. Jones,[2]
G. Kyrala,[2] S. Le Pape,[2] R. A. Lerche,[2] O. L. Landen,[2] T. Ma,[2] A. J. MacKinnon,[2]
M. A. McKernan,[2] M. J. Moran,[2] E. Moses,[2] D. H. Munro,[2] J. McNaney,[2] H. S. Park,[2]
J. Ralph,[2] B. Remington,[2] J. R. Rygg,[2] S. M. Sepke,[2] V. Smalyuk,[2] B. Spears,[2]
P. T. Springer,[2] C. B. Yeamans,[2] M. Farrell,[3] D. Jasion,[3] J. D. Kilkenny,[3] A. Nikroo,[3]
R. Paguio,[3] J. P. Knauer,[4] V. Yu Glebov,[4] T. C. Sangster,[4] R. Betti,[4] C. Stoeckl,[4]
J. Magoon,[4] M. J. Shoup III,[4] G. P. Grim,[5] J. Kline,[5] G. L. Morgan,[5] T. J. Murphy,[5]
R. J. Leeper,[6] C. L. Ruiz,[6] G. W. Cooper,[7] and A. J. Nelson[7]

[1]*Massachusetts Institute of Technology Plasma Science and Fusion Center, Cambridge,
Massachusetts 02139, USA*
[2]*Lawrence Livermore National Laboratory, Livermore, California 94550, USA*
[3]*General Atomics, San Diego, California 92186, USA*
[4]*Laboratory for Laser Energetics, University of Rochester, Rochester, New York 14623, USA*
[5]*Los Alamos National Laboratory, Los Alamos, New Mexico 87545, USA*
[6]*Sandia National Laboratory, New Mexico 87123, USA*
[7]*University of New Mexico, Albuquerque, New Mexico 87131, USA*

DT neutron yield (Y_n), ion temperature (T_i), and down-scatter ratio (*dsr*) determined from measured neutron spectra are essential metrics for diagnosing the performance of inertial confinement fusion (ICF) implosions at the National Ignition Facility (NIF). A suite of neutron-time-of-flight (nTOF) spectrometers and a magnetic recoil spectrometer (MRS) have been implemented in different locations around the NIF target chamber, providing good implosion coverage and the complementarity required for reliable measurements of Y_n, T_i, and *dsr*. From the measured *dsr* value, an areal density (ρR) is determined through the relationship ρR_{tot} (g/cm^2) = $(20.4 \pm 0.6) \times dsr_{10\text{-}12\,\text{MeV}}$. The proportionality constant is determined considering implosion geometry, neutron attenuation, and energy range used for the *dsr* measurement. To ensure high accuracy in the measurements, a series of commissioning experiments using exploding pushers have been used for *in situ* calibration of the as-built spectrometers, which are now performing to the required accuracy. Recent data obtained with the MRS and nTOFs indicate that the implosion performance of cryogenically layered DT implosions, characterized by the experimental ignition threshold factor (ITFx), which is a function of *dsr* (or fuel ρR) and Y_n, has improved almost two orders of magnitude since the first shot in September, 2010. © *2012 American Institute of Physics*. [http://dx.doi.org/10.1063/1.4728095]

I. INTRODUCTION

Hot-spot ignition planned at the National Ignition Facility (NIF) (Ref. 1) requires the formation of a round, high temperature hot spot surrounded by high fuel areal density (ρR). Experimental information about yield (Y_n), ion temperature (T_i), ρR, and ρR asymmetries are critical for diagnosing implosion performance and understanding how the fuel assembles. To obtain this information, a suite of neutron spectrometers has been implemented and extensively used on the NIF for measurements of the neutron spectrum in the energy range from 1.5 to about 20 MeV. This range covers all essential details of the neutron spectrum, allowing for the simultaneous determination of ρR, T_i, Y_n, and possible non-thermal features in the implosion. From the primary neutron spectrum, T_i and Y_n are determined, and from the ratio between down-scattered and primary neutrons, the down-scattered ratio (*dsr*) is determined, which is to the first order proportional to the fuel ρR. The neutron spectrometers are part of a neutron diagnostic suite,[2] which also includes the neutron activation diagnostic (NAD) system[3] for absolute yield and relative spatial yield variation measurements, and a neutron imaging system (NIS) (Ref. 4) for measurements of the spatial distribution of the primary and down-scattered neutron source.

The neutron spectrometers, which include several neutron time-of-flight (nTOF) detectors[5–7] and a magnetic recoil neutron spectrometer (MRS),[8–11] are fielded at different
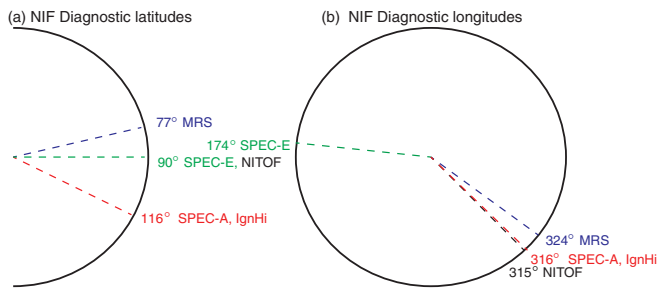
FIG. 1. Schematic drawings of the National Ignition Facility (NIF) chamber, indicating the different lines of sight (LOS) for the magnetic recoil spectrometer (MRS) and various neutron-time-of-flight (nTOF) neutron spectrometers. (a) Side projection. (b) Top view.

locations around the implosion for directional measurements of the neutron spectrum (Fig. 1). This ensures good coverage of the implosion, allowing for determination of ρR asymmetries[12] and possible non-thermal effects. The diametrically different detection principles of the MRS and nTOF techniques add to the reliability of the measurements.

To achieve the required accuracy for the measurement of the absolute neutron spectrum, a set of commissioning experiments was conducted on the NIF for an *in situ* calibration and characterization of the different spectrometers. With the spectrometers fully commissioned, they are now used routinely in support of the National Ignition Campaign (NIC).[13]

This paper is structured as follows. Section II describes the inertial confinement fusion (ICF) neutron spectrum. Aspects of the *dsr* measurement and how it relates to the total and Deuterium-Tritium (DT) fuel ρR are also discussed in this section. Section III discusses the neutron spectrometer commissioning experiments, and Sec. IV presents spectrometry data from cryogenically layered DT implosions.

II. THE ICF NEUTRON SPECTRUM

The ICF neutron spectrum has been described elsewhere,[5, 9, 12] and is therefore only discussed briefly in this paper. The D(T,n)α reaction produces primary neutrons with a kinetic energy of 14.03 MeV (zero temperature). As the DT reactions occur in a hot plasma, the primary neutron spectrum is Doppler broadened and energy upshifted due to a finite T_i. For a single-temperature plasma, T_i is determined from the Doppler width (ΔE_n^{FWHM}) of the primary neutron spectrum, which is well represented by a Gaussian distribution [T_i is to the first order equal to ($\Delta E_n^{FWHM}/177)^2$ keV].[14] Temperature profiles or non-thermal reactions result in deviations from the single-Gaussian distribution. Non-thermal effects could, for instance, be caused by bulk flows in the fuel at velocities as high as the speed of sound. Scattering in the cold, dense fuel and ablator that surrounds the hot spot gives rise to a low-energy (down-scattered) component in the neutron spectrum. The physical quantity measured by the neutron spectrometers is the down-scattered ratio, which is defined as $dsr(E) = Y(E)/Y_{n,13-15\ MeV}$, while hydrodynamic codes simulate compression performance given in ρR. Figure 2(a) shows neutron spectra simulated using the neutron transport code MCNPX (Ref. 15) for implosions with ρR varying from 0.1 to 2.0 g/cm^2. As shown, both shape and magnitude of
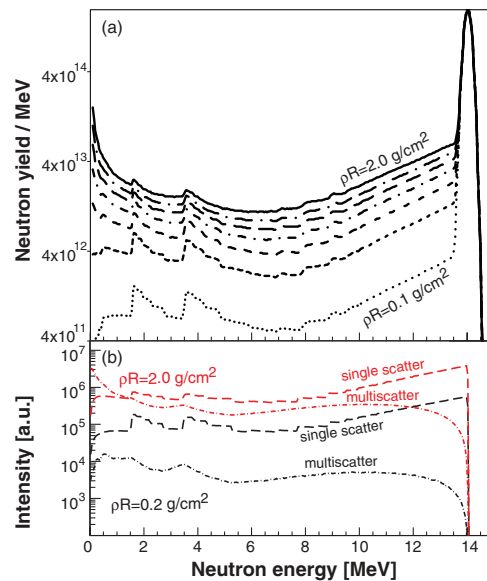

FIG. 2. (a) Simulated DT neutron spectra, normalized to a $Y_{n,13-15\ MeV}$ of 7×10^{14}. These simulations used a $T_i = 3$ keV DT primary-neutron point source in the center of a spherical high-density DT shell with inner and outer radii of 30 and 50 μm, and with varying ρRs (0.1, 0.4, 0.7, 1.0, 1.3, 1.6, and 2.0 g/cm^2). (b) Simulated single-scattered (dashed line) and multi-scattered (broken line) neutron spectra from a mono-energetic DT point source in a sphere with $\rho R = 0.2$ (black) and $\rho R = 2.0$ (red) g/cm^2. The (n,2n) reaction is also considered in these simulations. As can be seen, the multiple-scatter contribution increases significantly with ρR, especially at energies below $\sim$8 MeV.

the down-scattered neutron spectrum change significantly with increasing ρR. As discussed in Refs. 9, 12, and 16, the magnitude of the down-scattered neutron spectrum relative to the neutron yield, or *dsr*, is to the first order proportional to ρR. The conversion factor (C) between the fuel ρR and down-scatter ratio, $dsr(E) = Y(E)/Y_{tot}$ (where Y_{tot} is the total number of DT neutrons produced in the implosion), has been derived analytically[9] to be

$$\rho R_{DT}^{PS} \approx \frac{5m_p}{\sigma_{nd}(E) + \sigma_{nt}(E)} dsr(E) = C \times dsr(E), \quad (1)$$

where m_p is the proton mass and $\sigma(E)$ is the energy dependent cross sections for elastic *n,D* and *n,T* scattering and (n,2n) breakup reactions in D and T. These nuclear processes contribute to the measured low energy neutron spectrum and need to be included when integrating the cross sections over the appropriate energy interval. Eq. (1) is only valid for a point source (PS) and a 50:50 DT plasma. As the derivation of Eq. (1) only considers single scattering for a low ρR case, it needs to be modified to take into account (i) multiple scattering, (ii) attenuation of primary and down-scattered neutrons, (iii) the effect of ablator ρR, and (iv) the effect of implosion geometry (size and shape of the primary and scattering sources). As ρR increases, multiple scattering and attenuation become more significant at neutron energies below $\sim$8 MeV, resulting in a change in the spectral shape. This is shown in Fig. 2(b), which illustrates the single-scattering and multiple-scattering components for $\rho R = 0.2$ and $\rho R = 2.0$ g/cm^2 implosions. In addition, because multiple scattering and attenuation are significant in high-ρR implosions at the

NIF, the measured primary yield $Y_{n,\text{13-15 MeV}}$ does not well represent the total yield used in Eq. (1).

At bang time, some of the ablator mass needs to be preserved to control hydrodynamic instabilities in the implosion.[16] This remaining mass will contribute to the down-scattered neutron signal, but on a level much lower than the down-scattered neutron signal from the DT fuel. This is due to the smaller cross sections for the ablator material per mg/cm^2. If we assume a CH ablator (which is currently used on the NIF) and a relative ρR contribution from CH of $X = \rho R_{\text{CH}}/\rho R_{\text{DT}}$, then the fractional CH contribution to the observed $dsr_{\text{10-12 MeV}}$ can be written as

$$dsr_{\text{CH}} \approx \frac{5\sigma_{\text{CH}}(E)}{13\sigma_{\text{DT}}(E)} X \times dsr_{\text{DT}} \overset{\text{10–12 MeV}}{\approx} 0.12 X \times dsr_{\text{DT,10-12 MeV}}. \tag{2}$$

X has been estimated from simulations using the 2D hydro code LASNEX[17] to be ~ 0.1, which means that $\sim 1\%$ of the observed $dsr_{\text{10-12 MeV}}$ will be due to the CH ablator. This, however, means that the CH-ablator ρR is not well probed by down-scattered neutrons and needs to be measured in other ways, such as with knock-on protons,[18] gamma-ray spectroscopy,[19] or with x-ray methods.[20]

In realistic implosion geometries, the average neutron path length through the dense fuel is generally longer than the path length in the point-source case. This leads to higher measured dsr values for a given ρR, and a reduced conversion factor. LASNEX simulations of numerous NIF implosions were used to derive the following conversion factors for the total and fuel ρR:

$$\rho R_{\text{tot}}(\text{g/cm}^2) = (20.4 \pm 0.6) \times dsr_{\text{10-12 MeV}}, \tag{3}$$

$$\rho R_{\text{fuel}}(\text{g/cm}^2) = (18.8 \pm 0.5) \times dsr_{\text{10-12 MeV}}. \tag{4}$$

In these simulations, X was determined to be 0.08 ± 0.04.

The part of the implosion sampled by a spectrometer depends primarily on the dsr energy range used, composition of the fuel and ablator material, energy dependence of the differential cross section for the different nuclear processes, and implosion geometry. When only considering n,D and n,T elastic scattering (and not the (n,2n) processes), the sampled angular interval for a given scattered neutron energy range can be determined from the (non-relativistic) relationship

$$E_{n'} = \frac{1}{(A+1)^2} E_n (\cos\theta + (A^2 - \sin^2\theta)^{\frac{1}{2}})^2. \tag{5}$$

Here, $E_{n'}$ is the energy of the down-scattered neutron, θ is the neutron scattering angle in the lab system, and A the mass number of the scattered nucleus. Using Eq. (5), the sampled angular ranges for $E_{n'} = 10–12$ MeV and $E_{n'} = 6–12$ MeV can be illustrated for a neutron point source as in Fig. 3. For a more realistic implosion geometry, the fraction of the implosion sampled is increased relative to the point source case.

Currently, $E_{n'} = 10–12$ MeV is used for dsr measurements, but broader or different energy ranges have been used and will be routinely used in the near future. Ultimately, the plan is to use the whole neutron spectrum down to thermal energies[21] to extract as much information as possible about the implosion.
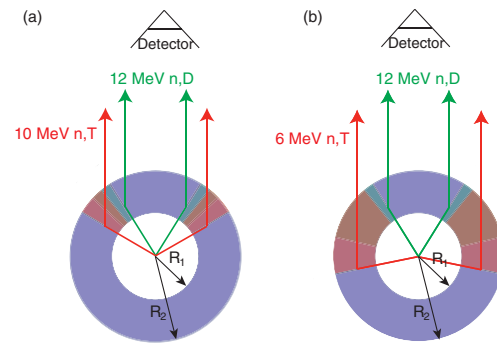

FIG. 3. Implosion region sampled when using (a) the $E_{n'} = 10–12$ MeV and (b) the $E_{n'} = 6–12$ MeV range for the dsr measurement. The implosion fraction sampled is 17% and 53% for 10–12 MeV and 6–12 MeV, respectively. For the determination of an average ρR that better represents the implosion performance, the 6–12 MeV energy range is preferable. These schematic drawings only consider single n,D elastic scattering (green), n,T elastic scattering (red), a point source, and a dense DT shell.

III. COMMISSIONING EXPERIMENTS

The different neutron spectrometers were installed and commissioned on the NIF in stages. The nTOFs were installed in 2009 and 2010, the MRS in late 2010, and the neutron imager time-of-flight (NITOF) in 2011. These spectrometers were commissioned over a time period of about 6–12 months, during which the systems were calibrated *in situ* in a coordinated fashion. In this section, the commissioning experiments are discussed in some detail. Common to all is that a series of exploding pusher implosions[22] was used to calibrate or verify the performance of the spectrometers before they were used to diagnose cryogenically layered DT implosions.

A. MRS

As the principle of the magnetic recoil neutron spectrometer (MRS) has been described in detail elsewhere,[8–11] it is only discussed briefly in this paper. The system consists of four main components: a 13 cm^2 deuterated polyethylene foil (CD$_2$) positioned 26 cm from target chamber center (TCC), a focusing magnet, made of Nd-Fe-B, positioned just outside the NIF chamber, an array of nine CR-39 detectors positioned at the magnet focal plane, and 6000 lbs of polyethylene shielding fully enclosing the spectrometer. The principle of the MRS is as follows. A small fraction of the emitted neutrons hit the CD$_2$ foil and produce elastically scattered deuterons. Forward-scattered deuterons are selected by an adjustable-sized magnet aperture positioned in front of the magnet. Selected deuterons are momentum analyzed and focused onto the CR-39 detector array. The position of the detected deuteron depends on its energy. The CR-39 detectors are processed in etch and scan labs, and then analyzed to reconstruct the recoil deuteron spectrum, from which the neutron spectrum is inferred (currently using a forward-fitting technique).

The efficiency of the MRS can be accurately calculated from first principles, allowing the MRS to provide a solid, independent Y_n measurement.[23] Spectral broadening due to geometry, CD$_2$ foil thickness, and magnet properties

determines the spectrometer resolution. In standard fashion, the efficiency can be increased at the expense of resolution by using a thicker CD_2 foil. To date, the MRS has been operated with six different foils, manufactured by General Atomics, ranging from ~50 to 250 μm in thickness. In addition, the MRS can be operated without a conversion foil for measurements of charged particles (e.g., 14.7 MeV protons from D^3He reactions) emitted directly from the implosion.

An accurate reconstruction of the neutron spectrum from the measured recoil-deuteron spectrum requires detailed knowledge about the instrument response function (IRF), which is calculated *ab initio* based on the MRS geometry and measured magnetic field map. The calculated IRF requires verification through *in situ* measurements to establish the as-built properties of the system. The MRS has been operated, without the CD_2 conversion foil, on D^3He Exploding Pusher shots N100823 (black circles) and N110722 (magenta crosses), Fig. 4(a). Solid calibration data were also obtained on a series of DT gas-filled exploding pushers (Fig. 4(b)). On DT shot N101030, the MRS was fielded in medium-resolution mode (~140 μm foil thickness, $\Delta E_{MRS} \approx 1100$ MeV full width half maximum (FWHM)), on DT shot N101212, it was fielded in medium-resolution mode with a 75 μm Ta ranging filter behind the foil to get a calibration point at ~8.5 MeV deuteron energy, and on DT shot N110217 it was fielded in high-resolution mode (~50 μm foil thickness, $\Delta E_{MRS} \approx 510$ MeV FWHM). It was found that this set of data could be described by simulations to an accuracy of ± 50 keV neutron energy equivalent if the magnetic field strength, as given by the manufacturer, Dexter Magnetic Technologies Inc., is increased by 4.95%.

The MRS was designed to minimize scattering materials between TCC and the CD_2 foil to avoid any background interference in the low-energy down-scattered neutron region, which could compromise the *dsr* measurement. It was also designed to reduce the ambient neutron background to the required level. Data from two DT exploding pushers (N101030 and N110217), in which the ρR is negligibly small, were used as a "null" test to ensure the quality of the MRS *dsr* measurement. The inferred $dsr_{10\text{-}12 \text{ MeV}}$ for N101030 and N110217 is $(0.1 \pm 0.1)\%$ and $(-0.2\% \pm 0.5)\%$, respectively, indicating that the background interference in the *dsr* measurement is insignificant.

B. nTOF

The suite of nTOF spectrometers includes a total of 12 instruments for diagnosing Deuterium-Deuterium (DD) and DT implosions.[5] In this paper, we focus on the nTOFs used for measurements of Y_n, T_i, and *dsr* in DT implosions. At this point, these include two liquid scintillators (Spec-A and Spec-E) at about 20 m from TCC, a set of chemical vapor deposition (CVD) diamonds at 20 m (IgHi), and a plastic scintillator at 27.3 m (NITOF). All nTOFs consist either of a fast CVD diamond or a scintillator detector coupled to a photodiode (PD) or photomultipler tube (PMT), biased to high voltage. Each nTOF is operated in current mode with the signal collected on one or more oscilloscopes. With a fixed and well-known
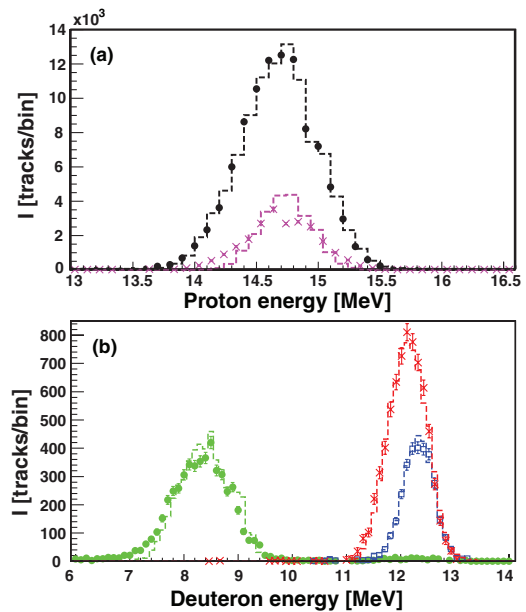

FIG. 4. (a) Measured spectra of D^3He protons coming directly from D^3He gas-filled exploding pusher shots N100823 (black circles) and N110722 (magenta crosses). No conversion foil was used for these measurements. (b) Measured recoil deuteron spectra for DT exploding pusher shots N101030 (red crosses), N110217 (blue squares), and N101212 (green circles). Simulations (overlayed dashed lines) reproduce the measured energy distributions over the full range to an accuracy of ± 50 keV neutron energy equivalent. Note deuterons fall at a location approximately corresponding to that of protons with double the energy due to the 2:1 mass ratio. See text for details.

distance to TCC and known IRF (discussed later), the neutron spectrum can be inferred from the time-of-flight signal.

Common to all these nTOF detectors is that an accurate absolute yield calibration could not be applied. Instead, they were cross-calibrated to the yield measured with the MRS and Zr and Cu neutron activation (NAD)[3] on DT exploding pushers. The yield calibration is continuously checked as new data are collected.

1. nTOF 20 m-SPEC detectors

The nominally identical Spec detectors, positioned 20 m from TCC in the neutron alcove (A) and on the equator (E), are the workhorse nTOF detectors designed to measure the neutron spectrum in the range 1.5–15 MeV and to provide accurate *dsr* and T_i measurements. They are oxygen-quenched xylene-based liquid scintillators[5] with a relatively narrow response (5 ns), coupled to two PMTs, PMT140 and PMT240, with different gain. The less-sensitive PMT140 (gain 10^3) is used to record the high-intensity neutron spectra from DT implosions, while the more-sensitive PMT240 (gain 10^5) is gated to only measure the spectrum below ~4 MeV, avoiding saturation from the 14-MeV neutrons.[6] The PMT140 is primarily used for the primary-neutron and 10–12 MeV *dsr* measurements. PMT240 is used to record the DD spectrum in a DT background and *n,D* and *n,T* elastic back-scatter edges (discussed in detail in Ref. 24).

To determine the IRFs for the Spec-A and Spec-E detectors, including cables, scintillators, and PMTs, an impulse response was first measured using an x-ray burst of
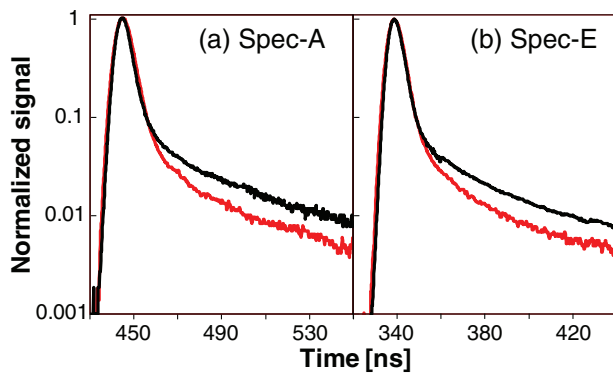
FIG. 5. (a) Neutron-time-of-flight (nTOF) Spec-A traces for a low-ρR exploding pusher (N111121, red) and a high-ρR DT layered shot (N111112, black). (b) Spec-E traces for the same shots. See text for details.
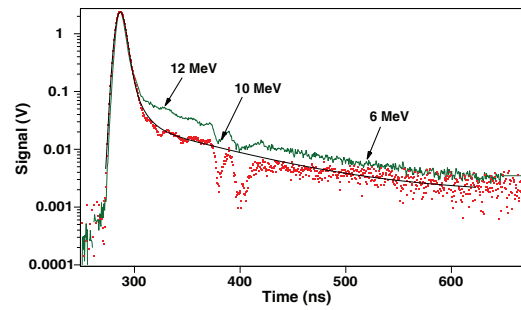

FIG. 6. Example of neutron imager time-of-flight (NITOF) data from DT Exploding Pusher shot N111121 (red) and DT layered shot N111215 (green, time shifted −20 ns to match N111121). The black curve represents the best-fit to the exploding pusher data using the IRF. The N111121 13–15 MeV intensity is renormalized to N111215. The intensity difference in the 6–12 MeV equivalent region (indicated in the figure) is due to down-scattered neutrons.

∼90 ps emitted from a planar-foil experiment on the NIF. For a complete characterization of the IRF, these impulse response measurements were convolved with the result from neutron transport and scintillator light yield calculations for 14 MeV neutrons in the lines of sight (LOS). In addition to the primary interaction with the scintillator, these calculations include the secondary generation of x-rays due to the interaction of neutrons with structures defining the LOS and structures surrounding the nTOF detector. The thus determined IRFs for Spec-A and Spec-E allow for an independent T_i measurement (accuracy ∼12%). The DT-primary signal decay (including contributions from scintillator afterglow, PMT response, and neutron scattering) was measured using "null ρR" DT exploding pushers to determine the background level for the *dsr* measurements on cryogenically layered DT shots. Figure 5 shows examples of nTOF Spec-A and Spec-E traces from a low-ρR exploding pusher (N111121) and a high-ρR layered DT shot (N111112). The difference in signal level in the time window 479–523 ns (Spec-A) and 370–410 ns (Spec-E), corresponding to 10–12 MeV neutrons, represents down-scattered neutron signal from the DT layered shot. The uncertainty in the *dsr* measurements is ∼10%, taking into account uncertainty in the exploding pusher baseline measurement.

2. nTOF 20 m-ignition high

The "ignition high" (IgHi) detector[5] is positioned 20 m from TCC in the neutron alcove. It consists of a set of four CVD diamonds of varying size and sensitivity. At current yields ($<10^{15}$), only the most sensitive diamond with 24 mm diameter and 1 mm thickness is providing good signal. IgHi has a very fast and narrow response (3.3 ns for the 24 mm detector, 1.2 ns for the 10 mm detectors), allowing for accurate T_i measurements. The IgHi IRF is constructed from x-ray response measurements using a diamond located at ∼4 m from TCC (nTOF BT[5]), convolved with the known IgHi cable response. As for the Spec-A and Spec-E detectors, the low-energy baseline signal is determined from DT exploding pusher measurements, allowing for a *dsr* determination from IgHi data (uncertainty ∼10%).

3. NITOF

The neutron imager time-of-flight (NITOF) detector is an NE-111 plastic-scintillator based detector fielded on the equator in the same LOS as the neutron imaging system at 27.3 m from TCC. The IRF (width 2.17 ns FWHM) is independently constructed from x-ray response measurements on the OMEGA laser facility (first decay constant), combined with scintillator decay property measurements using neutrons from an AmBe source at Los Alamos National Laboratory (LANL) (two longer decay constants).

DT exploding pusher data are accurately described by adjusting the width and amplitude of the IRF, as shown for N111121 in Figure 6, where data from layered shot N111215 are also shown for comparison. Unlike the other nTOF detectors, the NITOF low-energy baseline level is not determined from DT exploding pusher measurements. The background subtraction for the *dsr* measurement is done using data taken from equivalent out-of-beam detectors fielded on the same shot. The main background of scattered neutrons comes from the neutron imaging system itself. With its independent IRF calibration and unique scheme for *dsr* determination, NITOF adds important complementary *dsr* and T_i data (absolute accuracy 0.5% and 0.5 keV, respectively).

IV. DIAGNOSING CRYOGENICALLY LAYERED DT IMPLOSIONS

The suite of neutron spectrometers has been used to diagnose about 30 cryogenically layered implosions from the first dudded pre-tuning Tritium-Hydrogen-Deuterium (THD) implosions in 2010 and early 2011[25,26] through to the more recent 50:50 DT implosions in Uranium Hohlraums.

These measurements have been essential for diagnosing the implosion performance, characterized by the experimental ignition threshold factor (ITFx),[16,27,28] and for guiding NIC towards the first demonstration of ignition in a laboratory. The ITFx has improved from 1.5×10^{-3} on N100929 to ∼0.1 on N120321.

Figure 7(a) shows the primary neutron yield measured with the MRS compared to the weighted average yield measured with the NADs (including Cu and Zr NAD data) for
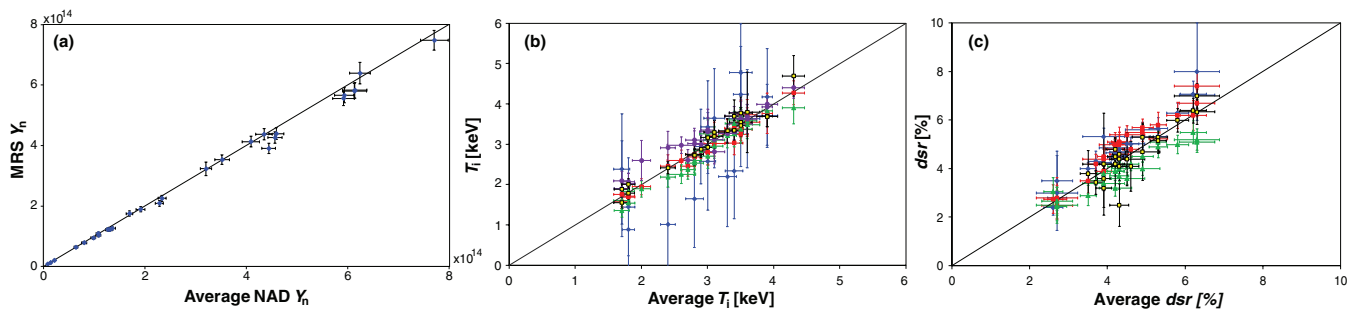
FIG. 7. (a) Primary neutron yield measured with the MRS as a function of the average yield measured with the NADs (blue diamonds) for DT layered shots, (b) Ion temperatures measured with MRS (blue diamonds), Spec-A (red squares), Spec-E (green triangles), IgHi (purple circles) and NITOF (black/yellow squares) as a function of the weighted average T_i for all layered DT shots, and (c) *dsr* (10–12 MeV) values measured with the MRS (blue diamonds), Spec-A (red squares), Spec-E (green triangles) and NITOF (yellow/black squares) as a function of the weighted average *dsr*. Also shown in each panel is the 45 line.

all layered shots. The plot shows consistent agreement over a large yield range.

As the IRFs for Spec-A, Spec-E, IgHi, NITOF, and MRS are independently determined, T_i results from these detectors are contrasted to the weighted average value in Fig. 7(b). The agreement between the Spec-A, Spec-E, and NITOF measurements is remarkable, given the different methods for determining the IRF. The error bars for MRS T_i data are large because the primary neutron yields have been $<10^{15}$, which requires the MRS to be operated in medium-resolution mode.

Figure 7(c) shows the *dsr* (10–12 MeV) data measured with the MRS, Spec-A, Spec-E, and NITOF as a function of the weighted average *dsr* value. As shown by the data, the SPEC-E *dsr* data are systematically lower than the *dsr* measured by the other spectrometers, which is most likely due to ρR asymmetries, but further investigations are required before any final conclusions can be drawn. The issue is currently being addressed by analyzing all the *dsr* data over a wider energy range, which corresponds to a larger coverage of the implosion (Fig. 3). This provides a better average ρR measurement. Using Eq. (3), the *dsr* values shown in the figure correspond to ρR values in the range 0.5–1.3 g/cm^2.

The individual measurements of Y_n, T_i, and *dsr* are weighted together, taking into account their errors, to get an average value that better represents the overall implosion performance. This average value is robust due to the large implosion coverage and the varying detection principles of the different instruments.

V. SUMMARY

A suite of neutron spectrometers, including an MRS and several nTOF detectors, has been implemented and extensively used on the NIF for measurements of the neutron spectrum in the energy range from 1.5 to about 20 MeV. The as-built performance of these spectrometers has been accurately calibrated using a series of DT and D^{3}He exploding pusher commissioning experiments. The spectrometers, which perform well and meet the required accuracies for the Y_n, T_i, and *dsr* measurements, have been essential for diagnosing the implosion performance of DT layered implosions and for guiding NIC towards the first demonstration of ignition in the laboratory.

[1]G. H. Miller, E. I. Moses, and C. R. Wuest, Nucl. Fusion **44**, S228 (2004).
[2]V. Yu. Glebov *et al.*, Rev. Sci. Instrum. **77**, 10E715 (2006).
[3]D. Bleuel, "Neutron Activation Diagnostics at the National Ignition Facility," Rev. Sci. Instrum. (these proceedings).
[4]F. E. Merrill, "The neutron imaging diagnostic at the National Ignition Facility," Rev. Sci. Instrum. (these proceedings).
[5]V. Yu. Glebov *et al.*, Rev. Sci. Instrum. **81**, 10D325 (2010).
[6]C. Stoeckl, M. Cruz, V. Yu. Glebov, J. P. Knauer, R. Lauck, K. Marshall, C. Mileham, T. C. Sangster, and W. Theobald, Rev. Sci. Instrum. **81**, 10D302 (2010).
[7]Z. A. Ali *et al.*, Rev. Sci. Instrum. **79**, 10E527 (2008).
[8]J. A. Frenje *et al.*, Rev. Sci. Instrum. **72**, 854 (2001).
[9]J. A. Frenje *et al.*, Rev. Sci. Instrum. **79**, 10E502 (2008).
[10]J. A. Frenje *et al.*, Phys. Plasmas **17**, 056311 (2010).
[11]D. T. Casey, "Diagnosing inertial confinement implosions at OMEGA and the NIF using novel neutron spectrometry," Ph.D. dissertation (MIT, 2012).
[12]D. C. Wilson, W. C. Mead, L. Disdier, M. houry, J.-L. Bourgade, and T. J. Murphy, Nucl. Inst. Meth. A **488**, 400 (2002).
[13]E. I. Moses, J. Phys.: Conf. Ser. **112**, 012003 (2008).
[14]H. Brysk, Plasma Phys. **15**, 611 (1973).
[15]MCNPX Version 2.5.0 User's Manual, LA-CP-05-0369, April 2005, see https://mcnpx.lanl.gov/
[16]M. J. Edwards *et al.*, Phys. Plasmas **18**, 051003 (2011).
[17]G. B. Zimmerman and W. L. Kruer, Comments Plasma Phys. Controlled Fusion **2**, 85 (1975).
[18]J. A. Frenje *et al.*, Phys. Plasmas **16**, 022702 (2009).
[19]N. M. Hoffman, D. C. Wilson, H. W. Herrmann, and C. S. Young, Rev. Sci. Instrum. **81**, 10D332 (2010).
[20]S. P. Regan, private communication (2012).
[21]S. L. Nelson, D. A. Shaughnessy, L. A. Bernstein, D. L. Bleuel, C. J. Cerjan, K. J. Moody, D. H. G. Schneider, and W. Stoeffl, IEEE Trans. Plasma Sci. **39**, 1750–1753 (2011).
[22]S. Le Pape *et al.*, Bull. Am. Soc. **56**, 192 (2011).
[23]D. T. Casey *et al.*, "Measuring the absolute DT neutron yield using the Magnetic Recoil Spectrometer at OMEGA and the NIF," Rev. Sci. Instrum. (these proceedings).
[24]C. Forrest *et al.*, "High resolution spectroscopy used to measure ICF neutron spectra on OMEGA," Rev. Sci. Instrum. (these proceedings).
[25]A. J. MacKinnon *et al.*, Phys. Rev. Lett. **108**, 215005 (2012).
[26]S. H. Glenzer *et al.*, Plasma Phys. Cont. Fusion **54**, 045013 (2012).
[27]B. Spears *et al.*, Phys. Plasmas **19**, 056316 (2012).
[28]S. H. Glenzer *et al.*, Phys. Plasmas **19**, 056318 (2012).